Molecular Phylogenetics and Evolution 161 (2021) 107182

Contents lists available at ScienceDirect

Molecular Phylogenetics and Evolution

journal homepage: www.elsevier.com/locate/ympev

Reticulate evolution in Conidae: Evidence of nuclear and mitochondrial introgression

Andrew W. Wood *, Thomas F. Duda Jr.

University of Michigan, Department of Ecology & Evolutionary Biology, 1105 North University Avenue, Biological Sciences Building, Ann Arbor, MI 48109-1085, USA

ARTICLE INFO

Keywords:
Conus
Introgression
Phylogeny
Adaptive radiation
Mito-nuclear discordance

ABSTRACT

Conidae is a hyperdiverse family of marine snails that has many hallmarks of adaptive radiation. Hybridization and introgression may contribute to such instances of rapid diversification by generating novel gene combinations that facilitate exploitation of distinct niches. Here we evaluated whether or not these mechanisms may have contributed to the evolutionary history of a subgenus of Conidae (*Virroconus*). Several observations hint at evidence of past introgression for members of this group, including incongruence between phylogenetic relationships inferred from mitochondrial gene sequences and morphology and widespread sympatry of many *Virroconus* species in the Indo-West Pacific. We generated and analyzed transcriptome data of *Virroconus* species to (i) infer a robust nuclear phylogeny, (ii) assess mitochondrial and nuclear gene tree discordance, and (iii) formally test for introgression of nuclear loci. We identified introgression of mitochondrial genomes and nuclear gene regions between ancestors of one pair of *Virroconus* species, and mitochondrial introgression between another pair. We also found evidence of adaptive introgression of conotoxin venom loci between a third pair of species. Together, our results demonstrate that hybridization and introgression impacted the evolutionary history of *Virroconus* and hence may have contributed to the adaptive radiation of Conidae.

1. Introduction

Reticulate evolutionary processes, such as introgressive hybridization, enable horizontal genetic exchange among otherwise independently evolving lineages and produce genomes comprised of genes with discordant patterns of descent (Doolittle, 1999; Pease and Hahn, 2015). As these processes are discovered at play across a widening cross-section of the tree of life (Abbott et al., 2013), interest has grown in understanding their role in the origin and maintenance of biodiversity. Species concepts have become more porous, and phylogenetic hypotheses now must account for the network-like patterns that reticulate processes can impart on evolutionary histories (Doolittle, 1999).

Lineages may be especially prone to introgressive hybridization during periods of rapid diversification in sympatry, conditions that are common during adaptive radiations (Seehausen, 2004). Conidae – "cone snails" – is a species rich (>900 species) (MolluscaBase eds., 2021) family of predatory marine gastropods that has likely experienced these conditions throughout its evolutionary history. This family has diversified rapidly over the past 55 million years, with the fastest diversification rate found in gastropods (Stanley, 2007). The genus *Conus* – which comprises about 85% of the described species of Conidae – has a circumtropical distribution with a center of diversity in the Indo-West Pacific where it is not uncommon to find many congeners coexisting in the same habitat, including an unusually high frequency of close relatives and sister species (Röckel et al., 1995; Kohn, 2001; Vallejo, 2005). Niche partitioning offers a possible mechanism for coexistence, with niche space partitioned according to diet with co-occurring species specializing on distinct prey taxa (Kohn, 1959; Leviten, 1978; Duda et al., 2009a).

The *Virroconus* clade stands out as one in which it would be fruitful to examine the role of reticulate processes in the diversification of *Conus*. It is comprised of thirteen species that have diversified in the past ~10 million years (Duda and Kohn, 2005), including some of the most widely distributed *Conus* species, and many coexist in the same microhabitats (Röckel et al., 1995; Kohn, 2001). Their relatively recent divergence and frequent sympatry suggest opportunities for hybridization. Moreover, conspicuous incongruence between mitochondrial phylogenies and relationships inferred from shell color patterns raises suspicions of reticulate evolution. Indeed, the species with different shell color patterns have been previously proposed to be members of distinct taxonomic

* Corresponding author at: The Pennsylvania State University, Department of Biology, 208 Curtin Road, Mueller Laboratory, University Park, PA 16802-5301, USA.
E-mail addresses: awwood@umich.edu, aww5450@psu.edu (A.W. Wood), tfduda@umich.edu (T.F. Duda).

https://doi.org/10.1016/j.ympev.2021.107182
Received 24 August 2020; Received in revised form 7 April 2021; Accepted 15 April 2021
Available online 20 April 2021

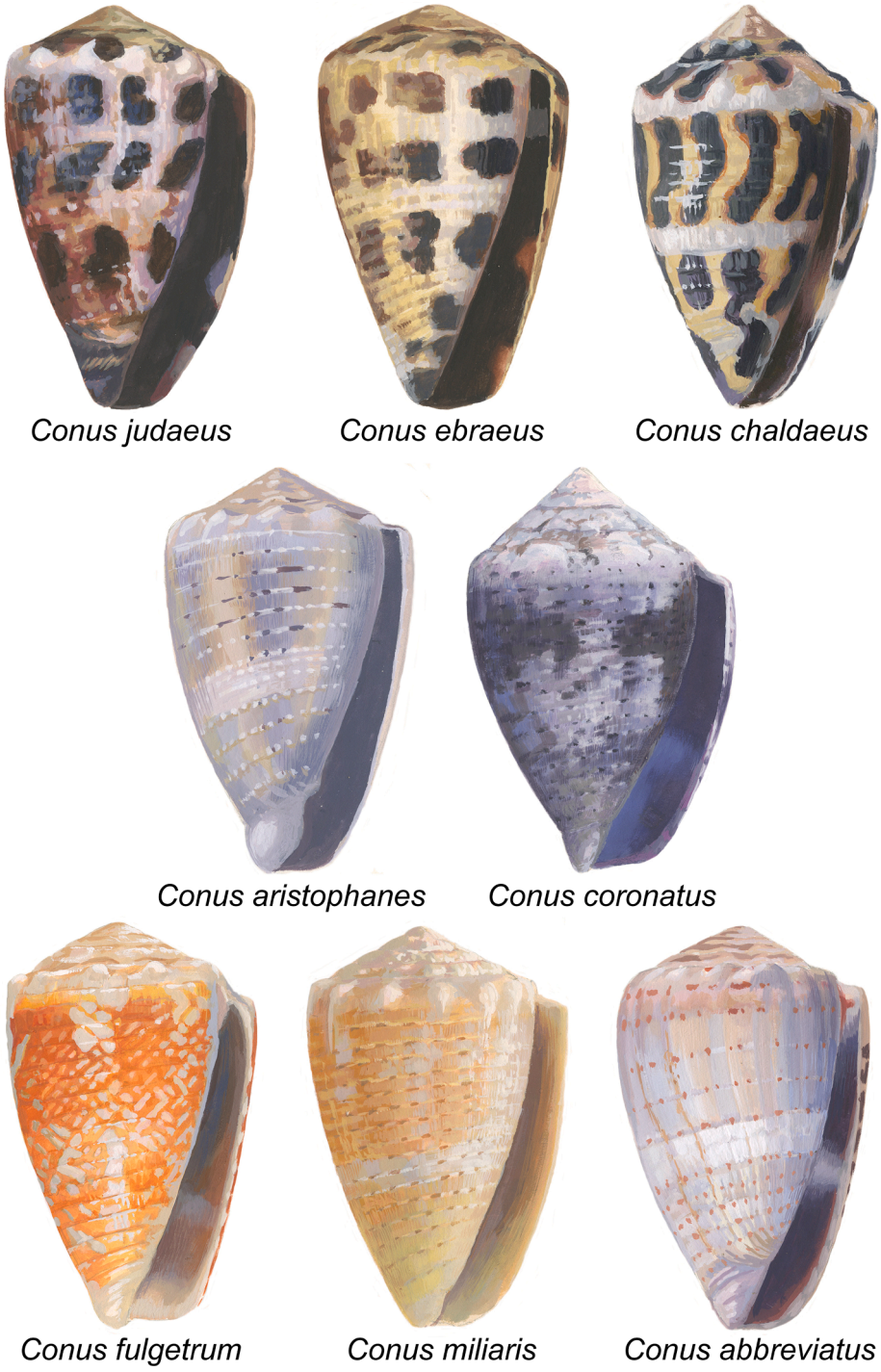

Fig. 1. Illustrations of *Virroconus* species with species sorted based on general similarity in shell color patterns. Illustrations by John Megahan.

groups (Tucker and Tenorio, 2009). Three pairs of species are of particular note: *Conus judaeus* – *Conus ebraeus*, *Conus aristophanes* – *Conus coronatus*, and *Conus fulgetrum* – *Conus miliaris* (Fig. 1). *Conus judaeus was* initially described by Rudolph Bergh (Bergh, 1895) from a single specimen collected in the Philippines (neotype at University of Michigan Museum of Zoology, UMMZ no. 303943), but was later synonymized with *C. ebraeus* by subsequent taxonomists due to the similar shell color patterns exhibited by these species (Fig. 1). The pattern of repeating black spots on a white background is a motif that is also shared by *Conus chaldaeus*, and that starkly contrasts with shell color patterns exhibited by other *Virroconus* members. Only after a comprehensive examination of radular morphology, feeding ecology, and sequence data was *C. judaeus* again recognized as a distinct species (Duda et al., 2009b). Although their color patterns suggest close phylogenetic affinity, mitochondrial gene sequences recovered from *C. ebraeus* and *C. judaeus* are relatively divergent, and phylogenies produced from these data recover *C. judaeus* as sister to *C. coronatus*, a species that has a quite different shell color pattern from those of *C. ebraeus* and *C. judaeus* (Fig. 1) (Remigio and Duda, 2008; Puillandre et al., 2014). This relationship is also surprising given the morphological similarity of *C. coronatus* and *C. aristophanes*, two species that have also historically been synonymized (Kohn, 1959) but that are not represented as sister species in phylogenies derived from mitochondrial genes (Remigio and Duda, 2008; Puillandre et al., 2014). These species are currently

Table 1
Summary of Conidae taxa sequenced.

Species	n	Tissue	Sex	Collection locale(s)
Conus miliaris	22	Venom duct	12♂, 10 ♀	Easter Island; Guam; American Samoa
Conus coronatus	2	Venom duct	2♀	American Samoa
Conus ebraeus	2	Venom duct	1♂, 1♀	Okinawa
Conus judaeus	2	Venom duct	1♂, 1♀	Okinawa
Conus chaldaeus	1	Osphradium	1♀	Okinawa
Conus abbreviatus	1	Venom duct	1♂	Hawaii
Conus aristophanes	2	Venom duct	1♂, 1♀	American Samoa
Conus fulgetrum	2	Venom duct	2♀	Okinawa
Outgroup spp.				
Conus mordeirae	2	Venom duct	1♂, 1 ♀	Cape Verde
Conus regonae	2	Venom duct	1♂, 1 ♀	Cape Verde

recognized as distinct species in MolluscaBase eds. (2021). A similar mismatch is apparent with *C. fulgetrum* and *C. miliaris*, the former having been identified at times as a subspecies of *C. miliaris* based on similarity in shell color patterns (Fig. 1) (Röckel et al., 1995). Yet again, although MolluscaBase currently synonymizes *C. fulgetrum* with *C. miliaris*, these species do not resolve as sister species in phylogenies constructed from analyses of mitochondrial gene sequences (Puillandre et al., 2014). Closer inspection of similar mismatches in other systems has frequently revealed that mitochondrial introgression is responsible (Shaw, 2002; Sota, 2002; Babik et al., 2005; Renoult et al., 2009; Köhler and Deein, 2010).

In this study we leveraged high-throughput RNA sequencing to generate a phylogenomic dataset for members of the *Virroconus* clade and used it to achieve three goals. First, we clarified the relationships of *Virroconus* species by building a robust phylogeny with a large set of nuclear orthologs. We then contrasted this phylogeny with one derived from mitochondrial data to map instances of mito-nuclear discordance in the clade that point to avenues of introgression. Finally, we formally tested for signatures of nuclear introgression among clade members.

2. Materials and methods

2.1. Taxon sampling

We sampled a total of 38 individuals from ten species: eight members of the *Virroconus* subgenus for which we had specimens (*Conus miliaris, Conus fulgetrum, Conus judaeus, Conus ebraeus, Conus aristophanes, Conus abbreviatus, Conus coronatus, Conus chaldaeus*), and two outgroup species (*Conus mordeirae* (=*Conus cuneolus* according to Tenorio et al. (2020) and MolluscaBase (2021)) and *Conus regonae*) from the Cape Verde species flock. For two species, *C. miliaris* and *C. coronatus*, we used sequence data that was previously generated from three distinct populations by Weese and Duda (2019), and were therefore able to include more individuals of *C. miliaris* (22) than the other species. The extra data available for *C. miliaris* facilitated a reference-based transcriptome assembly approach. Identifications of phenotypically similar *C. ebraeus* and *C. judaeus* had previously been confirmed using mtDNA sequences. We lacked appropriately preserved tissues from additional *Virroconus* species (i.e., *Conus dorreensis*, *Conus encaustus*, *Conus lecourtorum*, and *Conus taeniatus*), and so did not include them in our analyses. All tissues used in this study were retrieved from the University of Michigan Museum of Zoology (UMMZ) Mollusk Division collections, where tissues were stored in −80 °C or long-term liquid nitrogen storage. Specimens obtained, collection locales, sex, and tissue types are presented in Table 1.

2.2. RNA extraction, library preparation, & sequencing

We followed workflows described by Weese and Duda (2019) to generate transcriptome data. Total RNA was extracted from whole venom ducts for all specimens except *C. chaldaeus*, for which the osphradium (an olfactory organ) was utilized because a venom duct was not available. Consequently, data recovered from *C. chaldaeus* was not included in analyses involving conotoxin genes. In brief, tissues were pestle-homogenized and total RNA was extracted using Trizol (Invitrogen, Carlsbad, CA, USA) following the supplier instructions. RNA was submitted to the University of Michigan DNA Sequencing Core for quality assessment using a Bioanalyzer 2100 and for library preparation and indexing (Illumina Tru-Seq kit, San Diego, CA, USA). Samples were spread over three flowcell lanes on an Illumina HiSeq4000. Raw read data for *C. miliaris* is available from NCBI under BioProject number PRJNA257931, and for all other individuals under BioProject number PRJNA658056.

2.3. Read processing, transcriptome assembly, transcript filtering

To generate our phylogenomic dataset we built a robust *de novo* transcriptome of *C. miliaris* (the species with the highest quality data) which we then used as a scaffold for reference-based assembly of transcriptomes of the remaining species. We extracted a reliable set of orthologs from assembled transcriptomes using the phylogenomic dataset construction pipeline established by Yang and Smith (2014). A number of tools implemented in this pipeline are from Phyx (Brown et al., 2017). All analyses were performed on the University of Michigan Flux High Performance Computing core.

Raw Illumina reads were filtered in the same way for both *de novo* and reference-based assemblies. Potential sequencing errors were corrected with Rcorrector (Song and Florea, 2015), and reads that could not be corrected were removed. Trimmomatic v0.36 (Bolger et al., 2014) was used with default parameters to remove Illumina sequencing adapters and low-quality sequences. Reads were binned as mitochondrial or nuclear DNA according to whether or not they mapped to a custom database comprised of nine complete *Conus* mitochondrial genomes (none of them *Virroconus*) using Bowtie2 v2.3.4.3 (Langmead and Salzberg, 2012). FastQC v0.10.1 (Andrews, 2010) was used to assess read quality and read-representation; over-represented sequences were culled. Cleaned *C. miliaris* reads were then assembled *de novo* using Trinity v2.4.0 (Grabherr et al., 2011).

We stringently filtered the *C. miliaris* transcriptome to serve as a reference for assembling transcriptomes of other species. Assembly quality was assessed using Transrate v1.0.3 (Smith-Unna et al., 2016) and poor-quality transcripts were removed using default settings. Chimeric transcripts were also removed using the Yang and Smith (2014) pipeline. Corset v1.07 (Davidson and Oshlack, 2014) was used to cluster transcripts belonging to the same putative gene, and a single representative transcript–the largest in each cluster–was identified. Open reading frames (ORFs) were predicted using TransDecoder v5.0.1 (Haas et al., 2013) with a BLASTp homology search included for ORF retention criteria. Candidate ORFs were blasted against a custom reference database that included all *Conus*, *Lottia gigantia*, and *Alpysia californica* protein sequences from the NCBI non-redundant database; ORFs with BLASTp hits were retained. Finally, redundant transcripts were removed using CD-HIT-EST (Li and Godzik, 2006; Fu et al., 2012), with a sequence identity threshold of 0.99.

To assemble transcriptomes for the remaining nine species, we used the read mapping program Stampy v1.0.32 (Lunter and Goodson, 2011) with default settings to align reads from each species to the filtered *C. miliaris* reference. Although a variety of read-mapping tools are available, we chose Stampy for its high sensitivity and optimization for aligning reads with sequence variation relative to the reference (Thankaswamy-Kosalai et al., 2017). Output SAM files were then converted to coordinate-sorted BAM files using samtools v1.3.1 (Li et al., 2009), and assembled using Trinity v2.4.0 in genome-guided mode (Grabherr et al., 2011). To minimize potential cross-contamination introduced during sample preparation or sequencing, we ran all assemblies and fastq read

files (except those of *C. miliaris & C. coronatus* for which data were generated separately) through CroCo v1.1 (Simion et al., 2018) with default settings, which produces a meta-transcriptome from all samples, maps reads to it, and determines putative cross-contamination based on relative read-coverage. We removed all transcripts identified as contaminants. We then ran the remaining transcripts through the same filtering pipeline used on the *C. miliaris* reference transcriptome.

Because conotoxins are central to the feeding ecology of cone snails and have likely played a role in the adaptive radiation of this family, we examined conotoxin loci separately from non-conotoxin ("housekeeping") loci to determine if they exhibit markedly different topologies or patterns of introgression suggestive of adaptive introgression. We therefore separated the final transcript set into conotoxin and non-conotoxin loci by creating a local BLASTx database from all conotoxin sequences in the Conoserver database (Kaas et al., 2008, 2012) and extracting those transcripts that hit with an e-value of 1e-4 or lower.

Mitochondrial genes were assembled for each species from raw, unfiltered reads using NOVOPlasty (Dierckxsens et al., 2017). We used the coding sequences of all 13 protein-coding mitochondrial genes of *Conus betulinus* as seed sequences. We used the complete *C. betulinus* mitochondrial genome (Genbank accession: NC_039922) as the reference sequence. We performed separate NOVOPlasty runs with each of the 13 genes as a seed sequence for each species. Default parameters were used except that read length was set to 151, insert size to 150, and K-mer size of 23. The identity of resultant contigs were confirmed using BLASTx, and assembled contigs were aligned to the appropriate seed sequence using MUSCLE (Edgar, 2004) and manually edited in Seqotron (Fourment and Holmes, 2016).

2.4. Ortholog inference

Orthology was inferred using the pipeline developed by Yang and Smith (2014). First, homology inference was conducted for nuclear loci using coding sequences obtained during the transcript filtering step. Transcripts from all species were combined into a single FASTA file and subjected to all-by-all BLASTn (Altschul et al., 1990) to identify clusters of similar transcripts as candidate homologs. Raw BLASTn output was filtered according to a hit fraction cutoff of 50% coverage to produce tight clusters and high-quality alignments. The resulting clusters were input to MCL v.14-137 (Enright et al., 2002; van Dongen and Abreu-Goodger, 2012) to refine clusters using a minusLogEvalue of one and an inflation value of 1.5, with the output filtered to retain only homolog clusters with at least four species represented. Putative homolog clusters were then refined using the iterative tree-building and deep-paralog trimming method described by Yang and Smith (2014). We executed three rounds of homolog tree building with internal branch-length cutoffs of 0.5, 0.25, and 0.15 before building bootstrapped final homolog trees. Final orthologs were then inferred using the Maximum Inclusion approach, set to a minimum of four represented taxa. Final ortholog clusters were aligned using PRANK v.15080 (Löytynoja and Goldman, 2008) and trimmed using Phyx (Brown et al., 2017) for a minimum column occupancy of 0.6.

2.5. Phylogenetic analyses

2.5.1. Mitochondrial data

We selected eight protein coding genes (COI, ND1, ND2, ND3, ND4, ND4L, ND5, ATP6) that were recovered from all ten species to use as our final mitochondrial dataset. Single concatenated sequences were produced for each species, aligned using MUSCLE (Edgar, 2004), and manually inspected and trimmed in Seqotron. We used ModelFinder (Kalyaanamoorthy et al., 2017) to select the best fit substitution model according to BIC (TPM3u + F + R2), and conducted phylogenetic inference using IQ-TREE (Nguyen et al., 2015) with 1000 bootstrap replicates.

2.5.2. Nuclear loci

We inferred a species tree from our nuclear loci using a concatenated supermatrix of non-conotoxin ("housekeeping") orthologs. Orthologs were included in the supermatrix if they were recovered from at least six species and if the trimmed ortholog alignment was at least 100 nucleotides long, resulting in a total of 2216 orthologs. We partitioned the supermatrix by locus, allowing each partition to evolve under a different substitution model. Model selection was done separately for each partition using ModelFinder (Kalyaanamoorthy et al., 2017), and combined for all loci into a NEXUS partition file. We then ran multi-locus partitioned tree inference with IQ-TREE (Nguyen et al., 2015) with 1000 bootstrap replicates. We carried out two additional analyses to assess the consistency of support across the phylogeny. First, we calculated gene concordance factors (gCF) and site concordance factors (sCF) using IQ-TREE concordance analysis (Minh et al., 2018). The former metric represents the proportion of genes trees containing a given branch and the latter the number of individual sites supporting a given branch. Both metrics account for variable taxon coverage among gene trees. They offer an alternative to bootstrap values for measuring branch support and provide insight into discordance between gene-trees and the species-tree. Second, we randomly assigned the 2216 loci into eight subsets of 277 loci each, concatenated and partitioned each subset, and estimated phylogenies with IQ-TREE in the same way that we did for the full-concatenation supermatrix. By assessing several subsamples of genes, we sought to determine how robust the relationships that we recover in our full concatenation tree are to random effects. The number of subsets was chosen arbitrarily.

2.6. Concordance analysis & tests of introgression

To test for introgression we used two approaches: Bayesian Concordance Analysis (BCA) and Patterson's D-statistic. We targeted these approaches based on patterns of discordance that we observed between our mitochondrial and nuclear trees, as well the IQ-TREE concordance factors.

2.6.1. Bayesian concordance analysis

We carried out BCA with the coalescent-based BUCKy v1.4.4 (Ané et al., 2007; Larget et al., 2010) to more closely examine the patterns of discordance suggested by the mitochondrial and nuclear trees and by gCFs/sCFs calculated by IQ-TREE. The relative frequencies of gene tree topologies that are discordant with the primary concordance tree provide hints as to which process – incomplete lineage sorting (ILS) or introgression – may have produced the discordance. If ILS is responsible, discordant topologies should be recovered at roughly equal frequencies. Introgression, however, should bias the frequency of discordant gene tree topologies toward the topology that groups hybridizing species (e.g. Durand et al., 2011). Like with IQ-TREE concordance factor analysis, BUCKy uses individual gene trees as input and produces concordance factors (CF) to produce a primary concordance tree and common discordant topologies, but BUCKy requires that input loci share a common set of taxa (i.e., a gene that is represented by only nine of ten species will be excluded from the analysis). We therefore performed BCA separately on different taxon subsets to maximize the number of usable loci for each analysis. We targeted these analyses to detect evidence of introgression in three areas of discordance: within the '*ebraeus*' clade (subset: *C. ebraeus, C. judaeus,* and *C. chaldaeus*), between *C. judaeus* and *C. coronatus* (subset: *C. chaldaeus, C. judaeus, C. coronatus*), and within the '*miliaris*' clade (*C. miliaris, C. fulgetrum,* and *C. abbreviatus*). We restricted subset size to four taxa to maximize the number of shared loci and so we could calculate Patterson's D-statistic (which requires a four-taxon phylogeny) on the same subsets. *C. mordeirae* was used as the outgroup species for all analyses. We analyzed housekeeping loci for all subsets and separately analyzed conotoxin loci for those subsets with sufficient loci available (*judaeus-coronatus* subset, and *miliaris* clade).

For each taxon subset, we extracted orthologs with all target taxa

Table 2
Summary of bioinformatic filtering pipeline. Read and transcript counts are pooled by species.

Species	Raw reads	Filtered reads	Raw transcripts	Filtered transcripts	Supermatrix occupancy (2116 total)
Conus miliaris	241,403,636	190,152,238	238,284	28,631	93.5% (2072)
Conus coronatus	30,841,334	22,831,016	44,859	6931	73.6% (1630)
Conus ebraeus	27,552,422	9,820,911	11,494	1406	13.2% (293)
Conus judaeus	44,441,736	16,311,881	101,437	10,312	49.7% (1102)
Conus chaldaeus	24,162,240	9,691,346	189,156	22,216	84.7% (1878)
Conus abbreviatus	19,832,559	14,333,554	29,203	7916	83.3% (1847)
Conus aristophanes	32,548,924	18,073,252	36,224	9100	81.6% (1808)
Conus fulgetrum	24,064,654	9,133,846	158,382	8307	48.1% (1066)
Conus mordeirae	45,714,732	20,992,365	124,001	16,288	86.0% (1905)
Conus regonae	43,014,796	18,489,458	118,915	15,306	85.6% (1896)

represented and produced separate Bayesian trees for each locus using MrBayes 3.2.6 (Huelsenbeck and Ronquist, 2001; Ronquist and Huelsenbeck, 2003) with two runs of four chains each, 10,000,000 generations, a sample frequency of 1000 and a burn-in fraction of 0.25. We then used BUCKy to summarize the output tree files for each locus and create input files for the BCA analysis. Concordance factors were estimated using BUCKy with four separate chains and 10,000,000 generations with the alpha parameter set to one.

2.6.2. Patterson's D-statistic

We formally tested for introgression by calculating Patterson's D-statistic (Patterson et al., 2012) with the software package DFOIL (Pease and Hahn, 2015). Briefly, the approach counts the number of bi-allelic sites in a set of four taxa, and tallies the number that fit ABBA and BABA patterns which is then used to calculate the D-statistic and an accompanying p-value (Green et al., 2010; Durand et al., 2011). Significantly higher counts of one pattern over the other indicate introgression. We extracted ortholog alignments and concatenated them into a single supermatrix for each taxon subset using Phyx (Brown et al., 2017). Site counts were performed on concatenated alignments using the script fasta2dfoil.py, and Patterson's D-statistic analysis was run with the script dfoil.py in dstat mode. Taxon subsets were the same as those used for BCA.

3. Results

3.1. Taxon sampling, RNA extraction, & sequencing

We sampled a total of 38 individuals representing 10 species: eight members of the *Virroconus* subgenus (*Conus miliaris, Conus fulgetrum, Conus judaeus, Conus ebraeus, Conus aristophanes, Conus abbreviatus, Conus coronatus, Conus chaldaeus*), and two outgroup species (*Conus mordeirae, Conus regonae*) from the Cape Verde species flock. Specimens obtained, collection locales, sex, and tissue types are presented in Table 1.

3.2. Transcriptome assembly and ortholog inference

We produced a robust *de novo* transcriptome for *C. miliaris*, which we then used for reference-based assemblies of transcriptomes for the remaining species. Results of the read-filtering, transcriptome assembly, and transcript filtering pipeline are summarized in Table 2. Our *de novo C. miliaris* reference transcriptome assembly resulted in 238,284 unfiltered transcripts and 28,631 post-filtering transcripts. This is similar to the number of uniquely-annotated transcripts (25,131) discovered by Weese and Duda (2019) with the same dataset.

Using the phylogenomic dataset construction pipeline established by Yang and Smith (2014), we identified a total of 2216 orthologs with coding sequences at least 100 nucleotides long that were found in a minimum of six taxa. Taxon occupancy of the resulting supermatrix is summarized in Table 2. On average, species were represented by 69.9% of orthologs. This average was brought down by relatively low representation in three species: *C. judaeus* (49.7%), *C. fulgetrum* (48.1%), and especially *C. ebraeus* (13.2%).

3.3. Phylogenetic analyses

3.3.1. Mitochondrial phylogeny

We produced a concatenated alignment of eight mitochondrial genes that were recovered from all ten species (COI, ND1, ND2, ND3, ND4, ND4L, ND5, ATP6). The final alignment of 7846 nucleotides was input to IQ-TREE (Nguyen et al., 2015) to produce a maximum likelihood phylogeny (Fig. 2a). This tree presents a topology similar to those generated for *Virroconus* in prior studies that utilized mitochondrial sequence data (Remigio and Duda, 2008; Puillandre et al., 2014) and separates the group into two main clades. These groupings reproduce the incongruence between morphology and phylogeny noted previously, most obvious in the sister species relationship between *C. judaeus* and *C. coronatus*.

3.3.2. Nuclear phylogeny

We inferred a species tree from our nuclear loci using a concatenated supermatrix of non-conotoxin ("housekeeping") orthologs. The final nuclear supermatrix included 2216 loci and the concatenated alignment is 1,687,663 characters, with overall site occupancy of 63.7%. Site occupancy for *C. ebraeus* (13.2%) was markedly lower (Table 2). We used this alignment to produce a maximum likelihood phylogeny with IQ-Tree (Fig. 2b) that separates *Virroconus* into two main clades: the '*ebraeus*' clade and the remaining *Virroconus* species (the '*miliaris*' clade plus *C. coronatus* and *C. aristophanes*). Node support was assessed with 1000 bootstrap replicates and by calculating site and gene concordance factors (sCF and gCF, respectively). Although bootstrap values indicate mostly high branch support (with the exception of the sister pairing of *C. judaeus* and *C. ebraeus,* perhaps due to the small number of *C. ebraeus* loci), gCF and sCF values are less consistent and suggest reasonably high levels of gene tree discordance in some areas of the tree, particularly within the *ebraeus* and *miliaris* clades. These values do, however, provide robust support for splitting the *ebraeus* clade from other *Virroconus* members (gCF 99.3, sCF 99.3). Eight trees built with random 277-locus subsets exhibit uncertainty in the arrangement of the *ebraeus* clade, but otherwise broadly agree with the full-concatenation tree. Of the eight subsets, a plurality (four) recover the same topology as the full-concatenation tree. Three recover *C. ebraeus* as sister to *C. chaldaeus* (otherwise identical), and one places *C. ebraeus* basal to the rest of the *Virroconus*.

In contrast to the mitochondrial tree (Fig. 2a), the nuclear tree largely groups species that are morphologically similar. *C. judaeus* and *C. ebraeus* are recovered as sisters, as are *C. coronatus* and *C. aristophanes*, the latter pair falling out adjacent to the clade containing *C. miliaris, C. abbreviatus,* and *C. fulgetrum*.

3.4. Bayesian concordance analysis

We performed BCA to ask if introgression is responsible for patterns

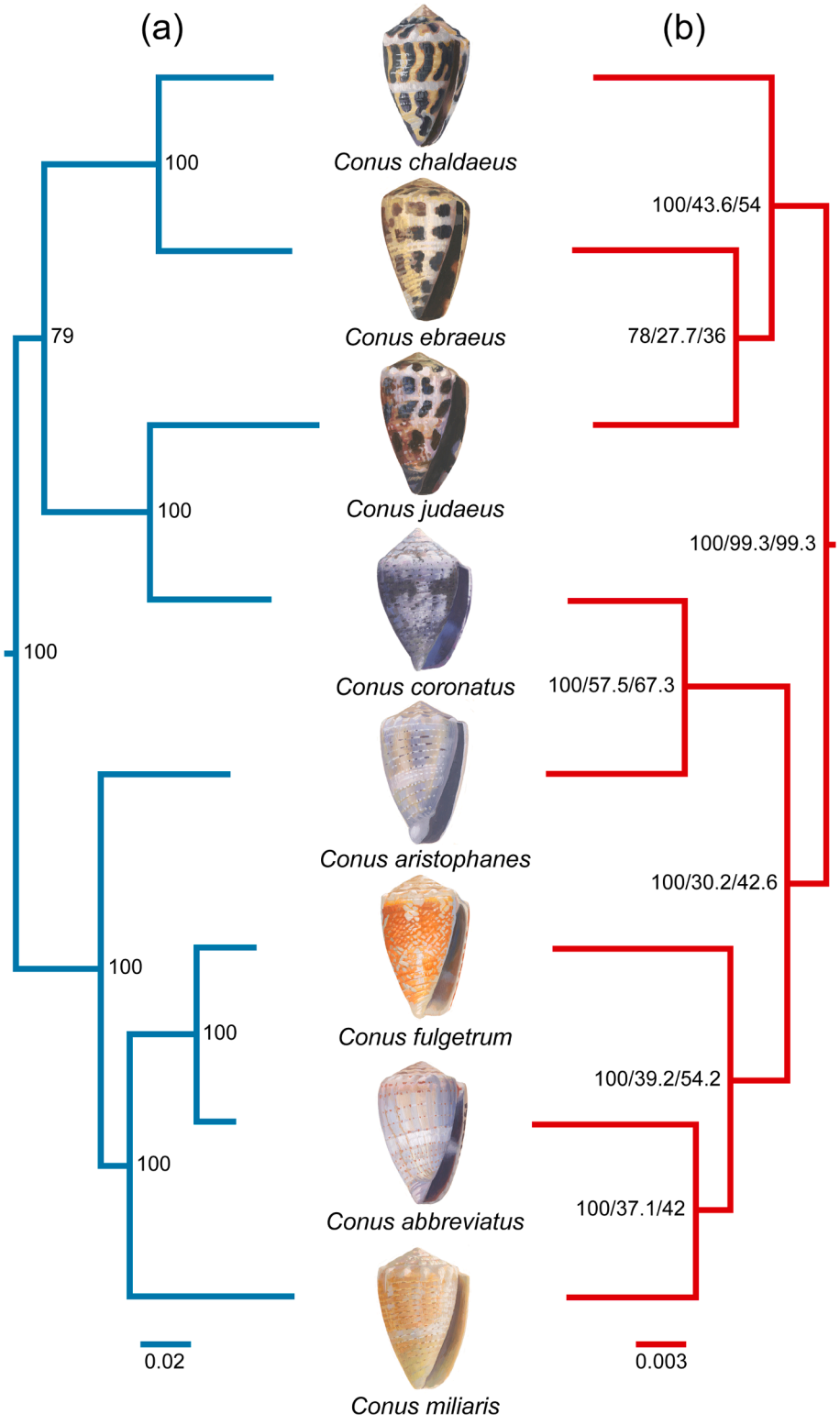

Fig. 2. Mitochondrial and nuclear phylogenies of *Virroconus*. **(a)** Maximum likelihood IQ-TREE phylogeny constructed from eight concatenated mitochondrial genes (blue topology). Bootstrap support values are presented at each node. **(b)** Maximum likelihood IQ-TREE phylogeny constructed from concatenated supermatrix of 2216 nuclear loci (red topology). Branch support values are indicated at each node (Bootstrap/gene concordance factor/site concordance factor). Both trees rooted using *C. regonae* and *C. mordeirae* as outgroups (not shown). Shell illustrations by John Megahan. (For interpretation of the references to color in this figure legend, the reader is referred to the web version of this article.)

of gene tree discordance (as opposed to ILS) in three subsets of *Virroconus* species. We analyzed housekeeping loci for all subsets, and separately analyzed conotoxin loci when possible.

BCA results do not show evidence of introgression among *C. ebraeus, C. chaldaeus*, and *C. judaeus* (Fig. 3a). Unlike our nuclear tree (Fig. 2b), the primary concordance tree generated by BCA recovers *C. chaldaeus* as sister to *C. ebraeus* as in the mitochondrial tree (Fig. 2a). However, the 95% confidence intervals of the concordance factors (CF) for all three possible topologies overlapped substantially, suggesting that the analysis was unable to resolve a confident primary concordance topology with the available loci. Due to the lack of venom duct tissue from *C. chaldaeus* and relatively low number of housekeeping loci recovered from *C. ebraeus*, we did not perform the corresponding BCA using conotoxin loci.

We found strong evidence of introgression between *C. judaeus* and *C. coronatus* (Fig. 3b) among housekeeping genes. Unlike the within-

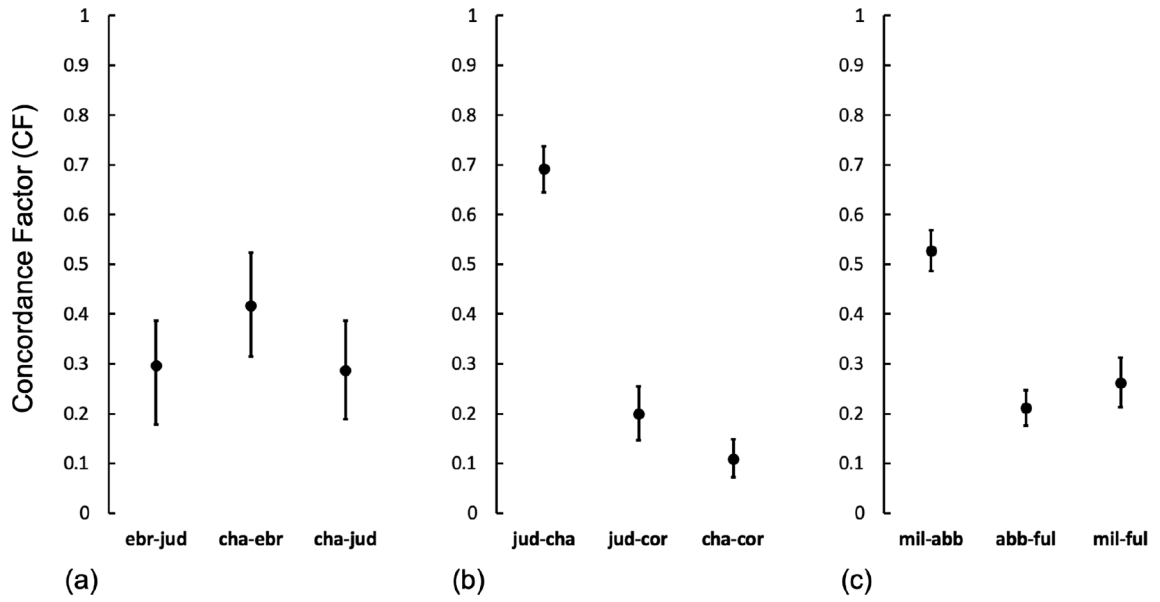

Fig. 3. Results of Bayesian concordance analysis conducted with BUCKy. Error bars show 95% confidence intervals (CI). **(a)** CFs of 111 housekeeping loci for the *ebraeus* clade. Overlapping confidence intervals for all topologies (including primary concordance tree) in the *ebraeus* clade show widespread discordance and no signal of introgression. **(b)** CFs of 470 housekeeping loci for the *judaeus-coronatus* taxon subset. High CF (CF = 0.692; CI: *0.645–0.738*) for the *C. judaeus-C. chaldaeus* pairing confirms the results of the nuclear phylogeny, and nearly non-overlapping CIs for the *C. judaeus-C. coronatus* (CF = 0.199; CI: *0.146–0.255*) and *C. chaldaeus-C. coronatus* (CF = 0.109; CI: *0.072–0.149*) pairings strongly suggest introgression between *C. judaeus* and *C. coronatus*. **(c)** CFs of 669 housekeeping loci for the *miliaris* clade. A distinctly higher CF (CF = 0.527; CI: *0.486–0.568*) for the *C. miliaris-C. abbreviatus* pairing confirms the results of the nuclear phylogeny. The CF for the *C. miliaris-C. fulgetrum* pairing (CF = 0.262; CI: *0.213–0.313*) is higher than for the *C. abbreviatus-C. fulgetrum* pairing (CF = 0.211; CI: *0.176–0.247*), but their CIs overlap substantially, and therefore do not strongly indicate introgression. All BCA used *C. mordeirae* as the outgroup species for tree-building.

ebraeus clade taxon subset, BCA for this subset confidently resolves a primary concordance tree in agreement with our nuclear tree (Fig. 2b), finding *C. chaldaeus* and *C. judaeus* to be sisters with a high CF (0.692) that does not overlap with discordant topologies. Moreover, the CF for the discordant *C. judaeus-C. coronatus* sister pairing (0.197) is higher than for *C. chaldaeus-C. coronatus* (0.093), with confidence intervals that

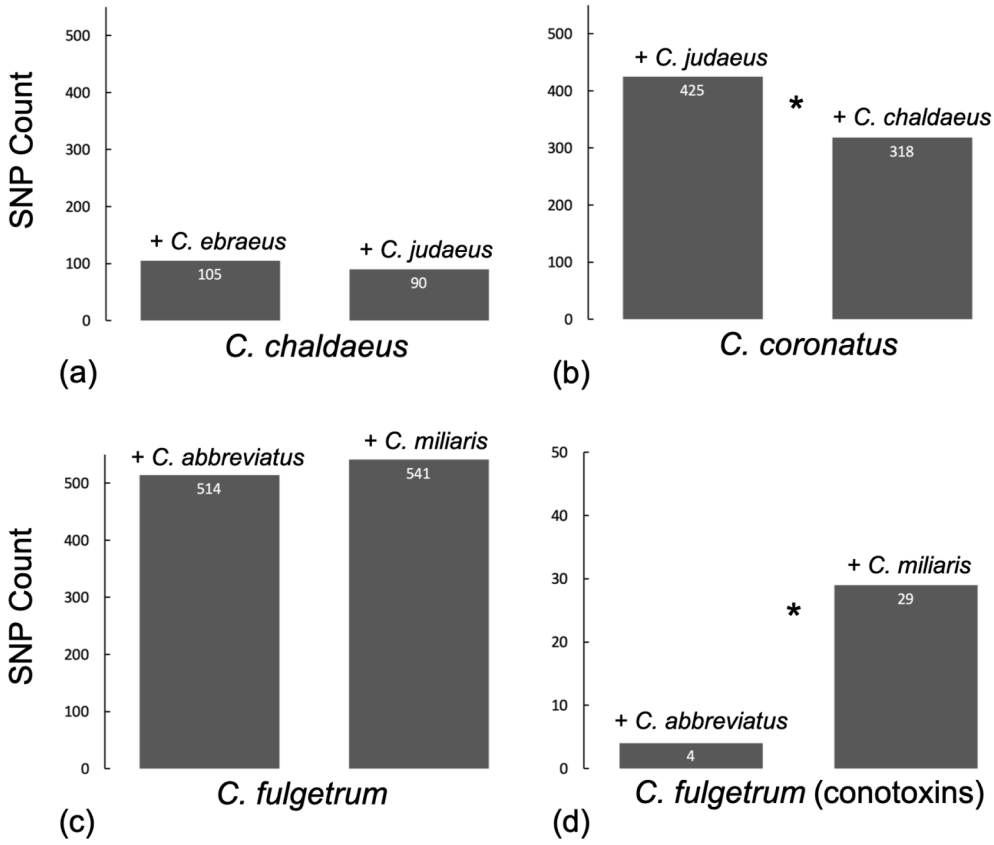

Fig. 4. D-statistic tests of introgression. Counts of SNPs with ABBA-BABA patterns are shown for each taxon subset are shown. The *ebraeus* clade **(a)** exhibits no evidence of introgression from *C. chaldaeus* among housekeeping loci ($D = 0.077$; *p-value* = 0.283). In the *judaeus-coronatus* subset **(b)** we recovered a significant D-statistic ($D = 0.144$; *p-value* = 8.66E−05) revealing introgression between *C. judaeus* and *C. coronatus*. The *miliaris* clade **(c)** shows no evidence of introgression from *C. fulgetrum* among housekeeping loci ($D = -0.026$; *p-value* = 0.406). Among conotoxin loci, the *miliaris* clade **(d)** exhibits significant evidence of introgression between *C. fulgetrum* and *C. miliaris* ($D = -0.758$; *p-value* = 1.35E−05). *C. mordeirae* was used as the outgroup species for all D-statistic calculations.

barely overlap. This strongly suggests that introgression between *C. judaeus* and *C. coronatus* and not ILS is responsible for the pattern of discordance we observe. When performed with conotoxin loci, the primary concordance tree again recovers *C. chaldaeus* and *C. judaeus* as sister species with a CF that does not overlap with the discordant topology. Due likely to the small number of shared conotoxin loci, only one of the possible discordant topologies was recovered, making it impossible to directly compare their frequencies. However, this topology has *C. judaeus* and *C. coronatus* as sister species, which is consistent with the evidence for introgression observed with housekeeping loci.

We do not see evidence of introgression among housekeeping genes among members of the *miliaris* clade (Fig. 3c). The primary concordance tree recovers *C. miliaris* and *C. abbreviatus* as sisters, consistent with our nuclear tree (Fig. 2b). Although the discordant topology pairing of *C. fulgetrum* with *C. miliaris* has a higher CF (0.262) than the topology pairing of *C. fulgetrum* with *C. abbreviatus* (0.211), the surrounding confidence intervals overlap substantially, failing to reject ILS as an explanation for the discordance. Our BCA using conotoxin loci for this subset produces a similar pattern as did the *judaeus-coronatus* taxon subset, recovering only one alternative topology (i.e., *C. fulgetrum* and *C. miliaris* as sister species). However, this topology is recovered as the primary concordance tree, with a higher CF than the tree pairing *C. miliaris* and *C. abbreviatus* as in the nuclear tree and BCA with housekeeping genes. Again, without the other discordant topology available, we cannot directly determine if introgression is responsible, but the results are consistent with the pattern observed in housekeeping genes and hint at a past history of introgression between *C. miliaris* and *C. fulgetrum*.

3.5. Patterson's D-statistic

To further examine the patterns observed in our concordance analyses and to formally test for introgression, we performed D-statistic analysis for the same taxon subsets as for BCA. In general, the results of this test corroborate patterns observed from BCA.

We do not find evidence of introgression of housekeeping genes among members of the *ebraeus* clade ($D = 0.077$; *p-value* $= 0.283$) (Fig. 4a). As with BCA, we were unable to calculate Patterson's D-statistic with conotoxin loci because we lacked venom duct tissue for *C. chaldaeus*. We detected strong evidence for introgression in the history of the *C. judaeus* and *C. coronatus* lineages ($D = 0.144$; *p-value* $=$ 8.66E−05) (Fig. 4b) as was suggested by patterns of discordance in mitochondrial and nuclear trees and BCA. We attempted to detect introgression among conotoxin loci by substituting *C. ebraeus* for *C. chaldaeus*, but there were too few of the required biallelic sites among the small number of shared loci to perform the analysis. We did not find introgression of housekeeping loci among members of the *miliaris* clade ($D = -0.026$; *p-value* $= 0.406$) (Fig. 4c), which is in line with results from BCA. We did, however, find evidence for introgression of conotoxin loci between *C. miliaris* and *C. fulgetrum* ($D = -0.758$; *p-value* $=$ 1.35E−05) (Fig. 4d). This finding is also consistent with the pattern we observed with conotoxin loci in BCA.

4. Discussion

Reticulate evolutionary processes such as introgressive hybridization play an under-explored role in the generation and maintenance of biodiversity. Such processes facilitate broader sampling of ancestral variation and can provide genetic raw material that underpins ecological specialization and fuels adaptive radiations (Toews and Brelsford, 2012). In this study, we used a phylogenomic dataset of 2216 loci to clarify the *Virroconus* phylogeny, detected strong mito-nuclear discordance, and identified several patterns of nuclear introgression, including one suggestive of adaptive introgression of conotoxin genes. Our results indicate that hybridization has played an active role in the evolutionary history of this group and demonstrate the viability of introgressive hybridization as a mechanism for genetic exchange among *Virroconus* and Conidae more broadly, further informing our understanding of the group's rapid diversification.

4.1. Mito-nuclear discordance & mitochondrial introgression

The phylogeny of *Virroconus* that we inferred from a robust phylogenomic dataset is markedly discordant with the topology of trees produced from mitochondrial loci (Fig. 2), both in this study and previously (Remigio and Duda, 2008; Puillandre et al., 2014). Similar patterns of mito-nuclear discordance are clear when comparing these mitochondrial phylogenies with the nuclear tree generated recently by Phuong et al (2019). Most immediately apparent is the rearrangement of *C. coronatus* and *C. judaeus*. While mitochondrial data recover these species as sisters in a clade positioned next to *C. ebraeus* and *C. chaldaeus*, our nuclear tree places *C. coronatus* and *C. aristophanes* as sister species and *C. judaeus* and *C. ebraeus* as sister species, and exhibits strong support for the node that separates members of the *ebraeus* clade from other *Virroconus* species (Fig. 2). This is strongly indicative of mitochondrial introgression between ancestors of *C. coronatus* and *C. judaeus*. We also detected discordance within the *miliaris* clade in terms of the relationships of *C. abbreviatus*, *C. fulgetrum*, and *C. miliairis*. While the mitochondrial tree reveals *C. abbreviatus* and *C. fulgetrum* as sister species, *C. abbreviatus* and *C. miliaris* are sister species in the nuclear tree. Both areas of mito-nuclear discordance–particularly involving *C. coronatus* and *C. judaeus*–suggest avenues by which other genetic variation, possibly adaptive, could have traversed species boundaries, an issue we explore further below.

In addition, our results support recognition of *C. fulgetrum* as a species that is distinct from *C. miliaris*, a result that was revealed previously by Puillandre et al. (2014) with mitochondrial sequence data and then later by Phuong et al. (2019) with nuclear sequence data. Although the trees presented in the supplementary materials of Phuong et al., show *C. miliaris* as two distinct lineages, one of the individuals represented in the tree is a specimen of *C. fulgetrum*, while the other presumably represents *C. miliaris*.

4.2. Nuclear introgression in Virroconus

We targeted three subsets of species for analyses of introgression based on initial patterns of discordance between nuclear and mitochondrial phylogenies. These analyses produced strong evidence for several patterns of nuclear introgression among *Virroconus* species, both expected and unexpected.

The pattern of introgression between *C. judaeus* and *C. coronatus* suggested by mitochondrial data was reinforced by our nuclear dataset. BCA and D-statistic tests both rejected ILS as an explanation for discordant topologies that pair *C. judaeus* and *C. coronatus* as sister species because the frequency of this topology is significantly higher than those that pair *C. chaldaeus* with *C. coronatus*. Such strong corroboration of the mitochondrial pattern of introgression from nuclear loci indicates hybridization between ancestors of *C. judaeus* and *C. coronatus*. The geographic distribution of these species offers one possible explanation for this pattern. Vallejo (2005) suggests that *Conus* underwent rapid speciation following the closure of the Tethys Sea, radiating eastwards from the Indo-West Pacific. *C. chaldaeus, C. ebraeus*, and *C. coronatus* all have widespread distributions throughout the Indo-West Pacific, with the two former species occurring in the eastern Pacific (Röckel et al., 1995); *C. judaeus*, however, is restricted to the Indian Ocean and western Pacific Ocean. Hybridization is thought to be linked with periods of rapid diversification (Seehausen, 2004). Our results suggest a scenario in which the Indian Ocean lineage of the common ancestor of the *ebraeus* clade hybridized with the ancestral lineage of *C. coronatus* during the period of rapid diversification that occurred after the closure of the Tethys, which ultimately led to the origin of *C. judaeus*.

Within the *miliaris* clade, our results hint at introgression among

housekeeping loci, but failed to reject ILS as an explanation. Nonetheless, we did find evidence of introgression of conotoxin loci between *C. miliaris* and *C. fulgetrum* based on analyses of Patterson's D-statistic. Unlike the *judaeus-ebraeus* taxon subset for which nuclear data reinforce the pattern of introgression suggested by mitochondrial data, in the *miliaris* clade the mitochondrial data suggest introgression between one species pair (*C. abbreviatus* and *C. fulgetrum*) while the nuclear conotoxin loci show introgression between another (*C. fulgetrum* and *C. miliaris*).

Despite substantial discordance within the *ebraeus* clade, we did not find evidence of introgression of housekeeping loci among these three species. Interestingly, the primary concordance tree produced by our BCA for this clade matches the topology inferred from our mitochondrial dataset and three of the random locus subset trees we inferred, placing *C. ebraeus* sister to *C. chaldaeus*. Together with the low IQ-TREE gCF values, these results leave the topology of the *ebraeus* clade unsettled. Such strong discordance may result from incomplete lineage sorting. However, our ability to confidently infer the relationships in this clade was handicapped by low ortholog recovery from the *C. ebraeus* transcriptome (13% ortholog representation). We need to examine a more complete *C. ebraeus* transcriptome before making inferences about the mechanism responsible for the nuclear discordance we observe in the *ebraeus* clade.

4.3. Morphology and discordance

The mitochondrial phylogeny produced largely recapitulates topologies inferred by previous studies that conflict with morphological variation present in *Virroconus*. The most striking of these are the sister species relationships inferred for *C. judaeus* and *C. coronatus* and to a lesser degree, *C. fulgetrum* and *C. abbreviatus* (Fig. 2a). Various aspects of shell morphology and coloration distinguish *C. judaeus* from *C. coronatus* (Fig. 1). Where the former is broadly conical, has a narrow aperture, and has a grid-like pattern of roughly parallelogram black spots, the latter is more ovate, with a wider aperture, and an irregular pattern of blotches of brown-black pigment punctuated with small spots that resemble dots and dashes (Röckel et al., 1995). *C. judaeus* and *C. ebraeus*, however, are indistinguishable using shell morphology alone, requiring inspection of radular teeth or DNA for reliable identification. Likewise, *C. fulgetrum* and *C. abbreviatus* have quite distinct shell patterning, each bearing some characteristics more similar to *C. miliaris*.

A shell collector arranging *Virroconus* species at a glance would almost certainly arrive at a different conclusion than the mitochondrial data, and our nuclear dataset would likely confirm her intuition, at least in part. The tree derived from our concatenated nuclear gene supermatrix resolves the incongruence between relationships inferred by mitochondrial gene trees and patterns of morphological variation. In particular, *C. judaeus* is united with *C. chaldaeus* and *C. ebraeus* in the *ebraeus* clade (Fig. 2b). In addition, *C. coronatus* is recovered as the sister species of *C. aristophanes* (Fig. 2b). Despite where taxon sampling differs, these results are concordant with the topology recovered by Phuong et al (2019).

These findings provide a useful roadmap that can be applied elsewhere in Conidae, which contains several cryptic species complexes. *Conus flavidus, Conus frigidus*, and *Conus peaseii*, for example, exhibit mito-nuclear discordance, and would benefit from a treatment utilizing multi-locus nuclear data (Lawler and Duda, 2017). More broadly, our results show that conflicts between relationships inferred from molecular phylogenies (especially those that use limited genetic data, such as mtDNA) and morphological variation warrants a richer genetic dataset to more completely reconstruct a group's evolutionary history and to determine if conflicts are due to introgression.

4.4. Implications for diversification in Conidae

Introgression provides avenues by which adaptive genetic variation may be exchanged among closely related species. Hybridization may therefore stimulate diversification and the origin of adaptations by producing novel gene combinations that enable occupation of different niches. The evolutionary impact of hybridization and introgression is highly context-dependent (Abbott et al., 2013), however, and the extent to which it affects broader macroevolutionary patterns and the generation of biodiversity is subject to debate (Seehausen, 2004; Mallet, 2007). Empirical and theoretical work suggest that the novel combinations of genetic and phenotypic variation produced by these processes are often deleterious (Mayr, 1963; Rieseberg, 1995), but when hybrid offspring encounter novel ecological conditions, such combinations may confer a fitness advantage or open previously inaccessible niches, thereby driving diversification (Anderson and Stebbins, 1954; Lewontin and Birch, 1966). The effects of this on evolutionary trajectories are increasingly well-documented and range from saltatory to incremental. Between 2% and 4% of angiosperm speciation events are estimated to have been the direct result of polyploidy resulting from hybridization, demonstrating the near instantaneous diversifying effects of hybridization (Otto and Whitton, 2000). Less dramatically, but perhaps more widespread, adaptive introgression has been found to combine beneficial alleles and accelerate diversification in a growing number of systems, including the Lake Victoria Region Superflock of cichlids (Meier et al., 2017), Caribbean pupfishes (Richards and Martin, 2017), and *Heliconius* bufferflies (Pardo-Diaz et al., 2012).

Venomous taxa are attractive systems to study how introgressed genes confer novel phenotypes, especially because single genes, or small cassettes of genes, may open entirely new dietary niches. In Mojave rattlesnakes, for example, the presence or absence of five genes dictates the difference between neurotoxic or hemorrhagic venom, with corresponding differences in prey (Strickland et al., 2018). In *Conus*, piscivory has evolved independently at least twice, and there are about 30 extant fish-eating *Conus* species (Duda and Palumbi, 2004). A worm-eating cone, *Conus tessulatus*, expresses a conotoxin peptide that is similar in sequence and function to conotoxins from fish-eating cones, which suggests that the peptide is an exaptation to a piscivorous feeding mode (Aman et al., 2015). If genes like those described in Mojave rattlesnakes and *C. tessulatus* were to leak through porous species boundaries, it is conceivable that they could open new ecological niches to their recipients. By revealing a history of hybridization in *Virroconus*, our study lays a foundation for future explorations of this possibility. Such studies could yield valuable insight into the diversification of Conidae, and the process of adaptive radiation more generally.

Funding

This work was supported by the University of Michigan Rackham Graduate Program and the University of Michigan Department of Ecology and Evolutionary Biology.

CRediT authorship contribution statement

Andrew W. Wood: Conceptualization, Methodology, Formal analysis, Visualization, Software, Investigation, Resources, Data curation, Writing - original draft, Writing - review & editing, Project administration, Funding acquisition. **Thomas F. Duda:** Conceptualization, Resources, Writing - review & editing, Supervision, Funding acquisition.

Acknowledgements

We would like to acknowledge the help of Dr. Taehwan Lee with retrieving specimens and collection data from the UMMZ collections. Dr. Raquel Marchán-Rivadeneira gave valuable guidance and support for the wet-lab work carried out for this project. Dr. Joe Walker provided essential help with the bioinformatic analyses, particularly the aspects involving Phyx.

Appendix A

See Table A1

Table A1
Detailed information for each sample utilized in this study. Tissue types are abbreviated as either venom duct (VD) or osphradium (O).

Sample code	Species	UMMZ catalog #	Sex	Tissue	Collection region	Collection locale	Latitude, Longitude	Collection date
CebrOK033	*Conus judaeus*	304718	F	VD	Okinawa, Japan	Cape Bise	26°42′33.9″N, 127°52′46.9″E	Jun. 25, 2015
CebrOK035	*Conus judaeus*	304720	M	VD	Okinawa, Japan	Cape Bise	26°42′33.9″N, 127°52′46.9″E	Jun. 25, 2015
CebrOK014	*Conus ebraeus*	304699	M	VD	Okinawa, Japan	Cape Bise	26°42′33.9″N, 127°52′46.9″E	Jun. 25, 2015
CebrOK016	*Conus ebraeus*	304701	F	VD	Okinawa, Japan	Cape Bise	26°42′33.9″N, 127°52′46.9″E	Jun. 25, 2015
CebrOK008	*Conus chaldaeus*	304693	F	O	Okinawa, Japan	Sesoko Station B	26°38′02.8″N, 127°51′51.0″E	Jun. 15, 2015
CabH073	*Conus abbreviatus*	302257	M	VD	Hawaii, USA	Maleakahana Beach Park	21°39′38.3″N, 157°55′39.9″W	Jul. 7, 2009
CabH075	*Conus abbreviatus*	302258	M	VD	Hawaii, USA	Maleakahana Beach Park	21°39′38.3″N, 157°55′39.9″W	Jul. 7, 2009
CcorAS019	*Conus aristophanes*	303201	M	VD	American Samoa, USA	Sliding Rock	14.35911°S, 170.779874°W	Apr. 6, 2010
CcorAS038	*Conus aristophanes*	303326	F	VD	American Samoa, USA	Sliding Rock	14.35911°S, 170.779874°W	Apr. 7, 2010
CantCV3	*Conus mordeirae*	300798	M	VD	Sal, Cape Verde	Algodoeira Beach	16.6166700°N, 22.95°W	Aug. 7, 2002
CantCV4	*Conus mordeirae*	300799	F	VD	Sal, Cape Verde	Algodoeira Beach	16.6166700°N, 22.95°W	Aug. 7, 2002
CregoCV5	*Conus regonae*	300822	F	VD	Sal, Cape Verde	North of Rigona	16.85°N, 22.93333°W	Aug. 11, 2002
CregoCV6	*Conus regonae*	300823	M	VD	Sal, Cape Verde	North of Rigona	16.85°N, 22.93333°W	Aug. 11, 2002
CmiliOK005	*Conus fulgetrum*	304875	F	VD	Okinawa, Japan	Sesoko Beach	26°39′00.4″N, 127°51′21.6″E	Jun. 22, 2015
CmiliOK006	*Conus fulgetrum*	304876	F	VD	Okinawa, Japan	Sesoko Beach	26°39′00.4″N, 127°51′21.6″E	Jun. 23, 2015
CmilAS023	*Conus coronatus*	303030	F	VD	American Samoa, USA	Fatumafuti	14.9°S, 170.7°W	Mar. 27, 2010
CmilAS045	*Conus coronatus*	303167	M	VD	American Samoa, USA	Tank Farm, Pago Pago Harbor	14.282522°S, 170.679554°W	Apr. 4, 2010
CmilEI120	*Conus miliaris*	302822	M	VD	Easter Island, Chile	Hanga Roa	27.1°S, 109.4°W	Nov. 2007
CmilEI165	*Conus miliaris*	302831	F	VD	Easter Island, Chile	Hanga Roa	27.1°S, 109.4°W	Nov. 2007
CmilEI202	*Conus miliaris*	302835	F	VD	Easter Island, Chile	Hanga Roa	27.1°S, 109.4°W	Nov. 2007
CmilEI283	*Conus miliaris*	302847	F	VD	Easter Island, Chile	Hanga Roa	27.1°S, 109.4°W	Nov. 2007
CmilEI329	*Conus miliaris*	302852	F	VD	Easter Island, Chile	Hanga Roa	27.1°S, 109.4°W	Nov. 2007
CmilEI381	*Conus miliaris*	302862	M	VD	Easter Island, Chile	Hanga Roa	27.1°S, 109.4°W	Nov. 2007
CmilEI388	*Conus miliaris*	302863	M	VD	Easter Island, Chile	Hanga Roa	27.1°S, 109.4°W	Nov. 2007
CmilEI400	*Conus miliaris*	302866	M	VD	Easter Island, Chile	Hanga Roa	27.1°S, 109.4°W	Nov. 2007
CmilGU075	*Conus miliaris*	302708	M	VD	Guam, USA	Pago Bay	13.4°N, 144.8°E	Jun. 10, 2008
CmilGU078	*Conus miliaris*	302709	F	VD	Guam, USA	Pago Bay	13.4°N, 144.8°E	Jun. 10, 2008
CmilGU085	*Conus miliaris*	302712	M	VD	Guam, USA	Pago Bay	13.4°N, 144.8°E	Jun. 10, 2008
CmilGU096	*Conus miliaris*	302715	F	VD	Guam, USA	Pago Bay	13.4°N, 144.8°E	Jun. 10, 2008
CmilGU100	*Conus miliaris*	302717	M	VD	Guam, USA	Pago Bay	13.4°N, 144.8°E	Jun. 10, 2008
CmilGU104	*Conus miliaris*	302719	F	VD	Guam, USA	Pago Bay	13.4°N, 144.8°E	Jun. 10, 2008
CmilGU117	*Conus miliaris*	302728	F	VD	Guam, USA	Pago Bay	13.4°N, 144.8°E	Jun. 10, 2008
CmilGU139	*Conus miliaris*	302733	M	VD	Guam, USA	Pago Bay	13.4°N, 144.8°E	Jun. 10, 2008
CmilAS014	*Conus miliaris*	303016	F	VD	American Samoa, USA	Fatumafuti	14.9°S, 170.7°W	Mar. 27, 2010
CmilAS027	*Conus miliaris*	303062	M	VD	American Samoa, USA	Fatumafuti	14.9°S, 170.7°W	Mar. 28, 2010
CmilAS028	*Conus miliaris*	303080	M	VD	American Samoa, USA	Fatumafuti	14.9°S, 170.7°W	Mar. 29, 2010
CmilAS032	*Conus miliaris*	303091	M	VD	American Samoa, USA	Fatumafuti	14.9°S, 170.7°W	Mar. 30, 2010
CmilAS035	*Conus miliaris*	303111	M	VD	American Samoa, USA	Fatumafuti	14.9°S, 170.7°W	Mar. 31, 2010
CmilAS038	*Conus miliaris*	303118	F	VD	American Samoa, USA	Fatumafuti	14.9°S, 170.7°W	Apr. 1, 2010

References

Abbott, R., Albach, D., Ansell, S., Arntzen, J.W., Baird, S.J.E., Bierne, N., Boughman, J., Brelsford, A., Buerkle, C.A., Buggs, R., et al., 2013. Hybridization and speciation. J. Evol. Biol. 26, 229–246.

Altschul, S.F., Gish, W., Miller, W., Myers, E.W., Lipman, D.J., 1990. Basic local alignment search tool. J. Mol. Biol. 215, 403–410.

Aman, Joseph, Imperial, Julita, Ueberheide, Beatrix, Zhang, Min-Min, Aguilar, Manuel, Taylor, Dylan, Watkins, Maren, Yoshikami, Doju, Showers-Corneli, Patrice, Safavi-Hemami, Helena, Biggs, Jason, Teichert, Russell, Olivera, Baldomero, 2015. Insights into the origins of fish hunting in venomous cone snails from studies of *Conus tessulatus*. Proc. Nat. Acad. Sci. U. S. A. 112 (16), 5087–5092. https://doi.org/10.1073/pnas.1424435112.

Anderson, E., Stebbins, G.L., 1954. Hybridization as an Evolutionary Stimulus. Evolution 8, 378–388.

Andrews S. 2010. FastQC: a quality control tool for high throughput sequence data. Available online at http://www.bioinformatics.babraham.ac.uk/projects/fastqc.

Ané, C., Larget, B., Baum, D.A., Smith, S.D., Rokas, A., 2007. Bayesian estimation of concordance among gene trees. Mol. Biol. Evol. 24, 412–426.

Babik, W., Branicki, W., Crnobrnja-Isailović, J., Cogălniceanu, D., Sas, I., Olgun, K., Poyarkov, N.A., Garcia-París, M., Arntzen, J.W., 2005. Phylogeography of two European newt species — discordance between mtDNA and morphology. Mol. Ecol. 14, 2475–2491.

Bergh, R., 1895. Beiträge zur Kenntnis der Coniden. *Nova Acta Kaiserl. Leopold.-Carol. deut Akad. Naturf* 65, 67–214.

Bolger, A.M., Lohse, M., Usadel, B., 2014. Trimmomatic: a flexible trimmer for Illumina sequence data. Bioinformatics 30, 2114–2120.

Brown, J.W., Walker, J.F., Smith, S.A., 2017. Phyx: phylogenetic tools for unix. Bioinformatics 33, 1886–1888.

Davidson, N.M., Oshlack, A., 2014. Corset: enabling differential gene expression analysis for de novoassembled transcriptomes. Genome Biol. 15, 410.

Dierckxsens, N., Mardulyn, P., Smits, G., 2017. NOVOPlasty: de novo assembly of organelle genomes from whole genome data. Nucleic Acids Res. 45, e18.

van Dongen S., Abreu-Goodger C. 2012. Using MCL to Extract Clusters from Networks. In: van Helden J., Toussaint A., Thieffry D. (Eds.), Bacterial Molecular Networks: Methods and Protocols. Methods in Molecular Biology. Springer New York, New York, NY, p. 281–295. Available from: https://doi.org/10.1007/978-1-61779-361-5_15.

Doolittle, W.F., 1999. Phylogenetic Classification and the Universal Tree. Science 284, 2124–2128.

Duda, T.F., Chang, D., Lewis, B.D., Lee, T., 2009a. Geographic variation in venom allelic composition and diets of the widespread predatory marine gastropod Conus ebraeus. PLoS One 4, e6245.

Duda, T.F., Kohn, A.J., 2005. Species-level phylogeography and evolutionary history of the hyperdiverse marine gastropod genus Conus. Mol. Phylogenet. Evol. 34, 257–272.

Duda, T.F., Kohn, A.J., Matheny, A.M., 2009b. Cryptic species differentiated in Conus ebraeus, a widespread tropical marine gastropod. Biol. Bull. 217, 292–305.

Duda, T.F., Palumbi, S.R., 2004. Gene expression and feeding ecology: evolution of piscivory in the venomous gastropod genus *Conus*. Proc. R. Soc. Lond. B Biol. Sci. 271, 1165–1174.

Durand, E.Y., Patterson, N., Reich, D., Slatkin, M., 2011. Testing for ancient admixture between closely related populations. Mol. Biol. Evol. 28, 2239–2252.

Edgar, R.C., 2004. MUSCLE: multiple sequence alignment with high accuracy and high throughput. Nucleic Acids Res. 32, 1792–1797.

Enright, A.J., Van Dongen, S., Ouzounis, C.A., 2002. An efficient algorithm for large-scale detection of protein families. Nucleic Acids Res. 30, 1575–1584.

Fourment, M., Holmes, E.C., 2016. Seqotron: a user-friendly sequence editor for Mac OS X. BMC Res. Notes 9, 106.

Fu, L., Niu, B., Zhu, Z., Wu, S., Li, W., 2012. CD-HIT: accelerated for clustering the next-generation sequencing data. Bioinformatics 28, 3150–3152.

Grabherr, M.G., Haas, B.J., Yassour, M., Levin, J.Z., Thompson, D.A., Amit, I., Adiconis, X., Fan, L., Raychowdhury, R., Zeng, Q., et al., 2011. Trinity: reconstructing a full-length transcriptome without a genome from RNA-Seq data. Nat. Biotechnol. 29, 644–652.

Green, R.E., Krause, J., Briggs, A.W., Maricic, T., Stenzel, U., Kircher, M., Patterson, N., Li, H., Zhai, W., Fritz, M.-H.-Y., et al., 2010. A draft sequence of the neandertal genome. Science 328, 710–722.

Haas B.J., Papanicolaou A., Yassour M., Grabherr M., Blood P.D., Bowden J., Couger M. B., Eccles D., Li B., Lieber M., et al. 2013. De novo transcript sequence reconstruction from RNA-Seq: reference generation and analysis with Trinity. Nat. Protoc. [Internet] 8. Available from: https://www.ncbi.nlm.nih.gov/pmc/articles/PMC3875132/.

Huelsenbeck, J.P., Ronquist, F., 2001. MRBAYES: Bayesian inference of phylogenetic trees. Bioinformatics 17, 754–755.

Kaas, Q., Westermann, J.-C., Halai, R., Wang, C.K.L., Craik, D.J., 2008. ConoServer, a database for conopeptide sequences and structures. Bioinformatics 24, 445–446.

Kaas, Q., Yu, R., Jin, A.-H., Dutertre, S., Craik, D.J., 2012. ConoServer: updated content, knowledge, and discovery tools in the conopeptide database. Nucleic Acids Res. 40, D325–D330.

Kalyaanamoorthy, S., Minh, B.Q., Wong, T.K.F., von Haeseler, A., Jermiin, L.S., 2017. ModelFinder: fast model selection for accurate phylogenetic estimates. Nat. Methods 14, 587–589.

Köhler, F., Deein, G., 2010. Hybridisation as potential source of incongruence in the morphological and mitochondrial diversity of a Thai freshwater gastropod (Pachychilidae, Brotia H. Adams, 1866). Zoosyst. Evol. 86, 301–314.

Kohn, A., 2001. Maximal species richness in Conus: diversity, diet and habitat on reefs of northeast Papua New Guinea. Coral Reefs 20, 25–38.

Kohn, A.J., 1959. The ecology of Conus in Hawaii. Ecol. Monogr. 29, 47–90.

Langmead, B., Salzberg, S.L., 2012. Fast gapped-read alignment with Bowtie 2. Nat. Methods 9, 357–359.

Larget, B.R., Kotha, S.K., Dewey, C.N., Ané, C., 2010. BUCKy: Gene tree/species tree reconciliation with Bayesian concordance analysis. Bioinformatics 26, 2910–2911.

Lawler, Alyssa, Duda Jr., Thomas, 2017. Molecular and morphometric data suggest the presence of a neglected species in the marine gastropod family Conidae. Mol. Phylogenet. Evol. 109, 421–429. https://doi.org/10.1016/j.ympev.2017.02.011.

Leviten, P.J., 1978. Resource partitioning by predatory gastropods of the Genus Conus on subtidal Indo-Pacific Coral Reefs: the significance of prey size. Ecology 59, 614–631.

Lewontin, R.C., Birch, L.C., 1966. Hybridization as a source of variation for adaptation to new environments. Evolution 20, 315–336.

Li, H., Handsaker, B., Wysoker, A., Fennell, T., Ruan, J., Homer, N., Marth, G., Abecasis, G., Durbin, R., 2009. The Sequence Alignment/Map format and SAMtools. Bioinformatics 25, 2078–2079.

Li, W., Godzik, A., 2006. Cd-hit: a fast program for clustering and comparing large sets of protein or nucleotide sequences. Bioinformatics 22, 1658–1659.

Löytynoja, Ari, Goldman, Nick, 2008. Phylogeny-aware gap placement prevents errors in sequence alignment and evolutionary analysis. Science 320 (5883), 1632–1635. https://doi.org/10.1126/science.1158395.

Lunter, G., Goodson, M., 2011. Stampy: A statistical algorithm for sensitive and fast mapping of Illumina sequence reads. Genome Res 21, 936–939.

Mallet, J., 2007. Hybrid speciation. Nature 446, 279–283.

Mayr, E., 1963. Animal Species and Evolution. Belknap Press of Harvard University Press, Cambridge, MA.

Meier, J.I., Marques, D.A., Mwaiko, S., Wagner, C.E., Excoffier, L., Seehausen, O., 2017. Ancient hybridization fuels rapid cichlid fish adaptive radiations. Nat. Commun. 8, 14363.

Minh B.Q., Hahn M.W., Lanfear R. 2018. New methods to calculate concordance factors for phylogenomic datasets. bioRxiv. 487801.

MolluscaBase eds. 2021. MolluscaBase. MolluscaBase [Internet]. Available from: http://www.molluscabase.org.

Nguyen, L.-T., Schmidt, H.A., von Haeseler, A., Minh, B.Q., 2015. IQ-TREE: a fast and effective stochastic algorithm for estimating maximum-likelihood phylogenies. Mol. Biol. Evol. 32, 268–274.

Otto, S.P., Whitton, J., 2000. Polyploid incidence and evolution. Annu. Rev. Genet. 34, 401–437.

Pardo-Diaz, C., Salazar, C., Baxter, S.W., Merot, C., Figueiredo-Ready, W., Joron, M., McMillan, W.O., Jiggins, C.D., 2012. Adaptive introgression across species boundaries in Heliconius Butterflies. PLoS Genet. 8, e1002752.

Patterson, N., Moorjani, P., Luo, Y., Mallick, S., Rohland, N., Zhan, Y., Genschoreck, T., Webster, T., Reich, D., 2012. Ancient admixture in human history. Genetics 192, 1065–1093.

Pease, J.B., Hahn, M.W., 2015. Detection and polarization of introgression in a five-taxon phylogeny. Syst. Biol. 64, 651–662.

Phuong, M.A., Alfaro, M.E., Mahardika, G.N., Marwoto, R.M., Prabowo, R.E., von Rintelen, T., Vogt, P.W.H., Hendricks, J.R., Puillandre, N., 2019. Lack of Signal for the Impact of Conotoxin Gene Diversity on Speciation Rates in Cone Snails. Syst. Biol. [Internet] https://academic.oup.com/sysbio/advance-article/doi/10.1093/sysbio/syz016/5366707.

Puillandre, N., Bouchet, P., Duda, T.F., Kauferstein, S., Kohn, A.J., Olivera, B.M., Watkins, M., Meyer, C., 2014. Molecular phylogeny and evolution of the cone snails (Gastropoda, Conoidea). Mol. Phylogenet. Evol. 78, 290–303.

Remigio, E.A., Duda, T.F., 2008. Evolution of ecological specialization and venom of a predatory marine gastropod. Mol. Ecol. 17, 1156–1162.

Renoult, J.P., Geniez, P., Bacquet, P., Benoit, L., Crochet, P.-A., 2009. Morphology and nuclear markers reveal extensive mitochondrial introgressions in the Iberian Wall Lizard species complex. Mol. Ecol. 18, 4298–4315.

Richards, E.J., Martin, C.H., 2017. Adaptive introgression from distant Caribbean islands contributed to the diversification of a microendemic adaptive radiation of trophic specialist pupfishes. PLoS Genet. 13, e1006919.

Rieseberg, L.H., 1995. The role of hybridization in evolution: old wine in new skins. Am. J. Bot. 82, 944–953.

Röckel, D., Korn, W., Kohn, A.J., 1995. Manual of the Living Conidae. Indo-Pacific Region, Hemmen.

Ronquist, F., Huelsenbeck, J.P., 2003. MrBayes 3: Bayesian phylogenetic inference under mixed models. Bioinformatics 19, 1572–1574.

Seehausen, O., 2004. Hybridization and adaptive radiation. Trends Ecol. Evol. (Amst.) 19, 198–207.

Shaw, K.L., 2002. Conflict between nuclear and mitochondrial DNA phylogenies of a recent species radiation: What mtDNA reveals and conceals about modes of speciation in Hawaiian crickets. Proc. Natl. Acad. Sci. USA 99, 16122–16127.

Simion, P., Belkhir, K., François, C., Veyssier, J., Rink, J.C., Manuel, M., Philippe, H., Telford, M.J., 2018. A software tool 'CroCo' detects pervasive cross-species contamination in next generation sequencing data. BMC Biol. [Internet] 16. https://www.ncbi.nlm.nih.gov/pmc/articles/PMC5838952/.

Smith-Unna, R., Boursnell, C., Patro, R., Hibberd, J.M., Kelly, S., 2016. TransRate: reference-free quality assessment of de novo transcriptome assemblies. Genome Res. 26, 1134–1144.

Song, L., Florea, L., 2015. Rcorrector: efficient and accurate error correction for Illumina RNA-seq reads. GigaScience 4, 48.

Sota, T., 2002. Radiation and reticulation: extensive introgressive hybridization in the carabid beetles Ohomopterus inferred from mitochondrial gene genealogy. Popul. Ecol. 44, 0145–0156.

Stanley, S.M., 2007. An analysis of the history of marine animal diversity. Paleobiology 33, 1–55.
Strickland, J.L., Smith, C.F., Mason, A.J., Schield, D.R., Borja, M., Castañeda-Gaytán, G., Spencer, C.L., Smith, L.L., Trápaga, A., Bouzid, N.M., et al., 2018. Evidence for divergent patterns of local selection driving venom variation in Mojave Rattlesnakes (Crotalus scutulatus). Sci. Rep. 8, 17622.
Tenorio M.J., Abalde S., Pardos-Blas J.R., Zardoya R. 2020. Taxonomic revision of West African cone snails (Gastropoda: Conidae) based upon mitogenomic studies: implications for conservation. EJT [Internet]. Available from: https://europeanjournaloftaxonomy.eu/index.php/ejt/article/view/975.
Thankaswamy-Kosalai, S., Sen, P., Nookaew, I., 2017. Evaluation and assessment of read-mapping by multiple next-generation sequencing aligners based on genome-wide characteristics. Genomics 109, 186–191.
Toews, D.P.L., Brelsford, A., 2012. The biogeography of mitochondrial and nuclear discordance in animals. Mol. Ecol. 21, 3907–3930.
Tucker, J., Tenorio, M., 2009. Systematic Classification of Recent and Fossil Conoidean Gastropods. Conchbooks, Hackenheim.
Vallejo, B., 2005. Inferring the mode of speciation in Indo-West Pacific Conus (Gastropoda: Conidae). J. Biogeogr. 32, 1429–1439.
Weese, D.A., Duda, T.F., 2019. Effects of predator-prey interactions on predator traits: differentiation of diets and venoms of a marine snail. Toxins 11, 299.
Yang, Y., Smith, S.A., 2014. Orthology inference in nonmodel organisms using transcriptomes and low-coverage genomes: improving accuracy and matrix occupancy for phylogenomics. Mol. Biol. Evol. 31, 3081–3092.